Towards Multiphase Modeling of Inhomogeneities in Mixers

Samia Shaikh *and Robert Prosser †

Abstract—**This paper is preliminary study to model flow within a multiphase mixer. This was achieved by primarily modeling a single liquid, which was validated by a grid independence and experimental PIV tests. A VOF model was simulated using the same agitator and vessel. Two modes of motion were found and the presence of local inhomogeneities through statistical analysis. Further work is required to model the mixture using Eulerian Multiphase Modeling.**

Keywords: Mixers, PIV, VOF, Multiphase

1 Introduction

Mixing occurs widely throughout different industries, such as chemical[1], pharmaceuticals[2] and food[3]. It can occur in just one phase or in many phases. Liquid mixing is a reasonably well understood and researched area; solid mixing on the other hand is not very well understood[4]. One of the main problems encountered with solid mixing is that of mixture homogeneity. The problem examined in this paper is based on an industrial mixing problem. The mixture is composed of many different constituents; particulates, flakes, fibres and some viscous liquids. The industrial partners current mixer configuration yields inhomogeneities in the mixture, which in turn is causing some wastage in the end product. The work presented in this paper is working towards an improved understanding of solid mixing, and to reduce mixture inhomogeneity in an industrial mixer.

Section 2 will examine the experimental method used to map out the mixer flow pattern and the numerical model used to model the flow. Section 3 will discuss the conclusions from the numerical and experimental tests. Section 4 discusses the ongoing work.

*The University of Manchester, Department of M.A.C.E. Sackville Street, Manchester, M60 1QD. Email: samia.shaikh@yahoo.co.uk

†The University of Manchester, Department of M.A.C.E. Sackville Street, Manchester, M60 1QD. Email: Robert.Prosser@manchester.ac.uk

2 Experimental and Numerical Studies

2.1 Experimental Method

In order to understand flow inhomogeneities, method must be adopted that allows the velocity mapping of the mixture non-intrusively. For a dense and opaque mixture this can be done be either using non-intrusively using electrical impedance tomography (EIT), electrical resistance tomography (ERT) or gamma ray tracking[4]. Based on the assumption that on a macro scale the liquid mixture will follow the same path as the solid mixture, a liquid system can used in order to map the flow field of the mixer. This can be done by using a particle image velocimetry system, which is a non-intrusive measurement method[5]. After obtaining experimental data from the simple liquid case, the next step is to study the actual solid mixture. As mentioned earlier this can be done either using EIT, ERT or gamma ray tracking.

The first step towards understanding solid mixing was to model the agitator in a simple liquid case. This was done for two reasons; to validate the numerical calculations and to identify any problem areas in the mixer, such as dead spots.

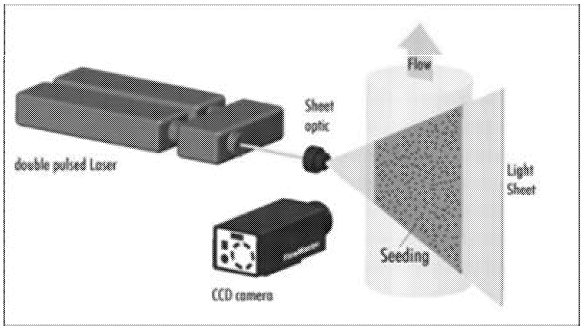

Figure 1: PIV system (courtesy of La Vision)

PIV(figure 1) units were supplied by La Vision and TSI. The PIV supplied was a 2 dimensional unit, which consisted of a class 4 Nd-Yag pulsed laser, a ccd camera and a data acquistion system. The mixer tank and the outer holding tank were made of perspex and the agitator was made of aluminium. The model tank was based on the original mixer configuration; flow conditions and mixer geometry were determined by dynamic and kine-

matic similarity calculations. Two blade configurations were used (figure 2); a simple blade and complex blade system. The complex blade system is mainly of interest to us in this study.

Figure 2: (a)Simple blade (b)Complex blade configuration

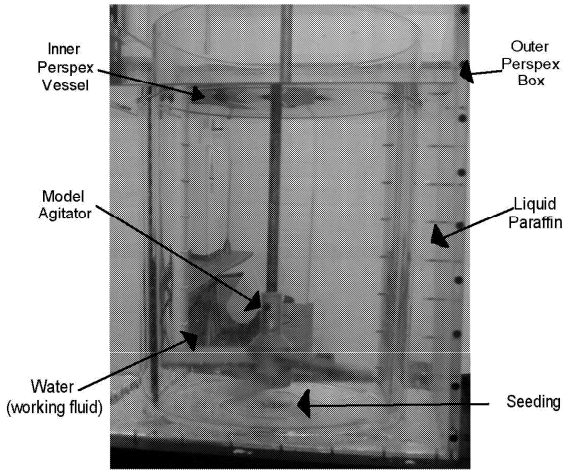

Figure 3: Experimental setup

The mixer tank was placed inside the holding tank, and the holding tank was then filled with glycerol in order to counter refraction effects (figure 3). The working liquid used in the mixer consisted of water. The liquid was initially seeded with fluorescene particles and agitated with the mixer blade. The flow was illuminated twice by the laser pulses and the light scattered by the particles was recorded on a series of frames. The distance travelled by the particles was determined by evaluating the images, which was in turn used to determine the velocity field of the mixture. Once all the data was obtained by the PIV system, it was analysed by the post processing software supplied by TSI and La Vision.

2.2 Numerical Model

2.2.1 Case A-Single Liquid Case

If the solid is assumed to be Newtonian and behaves like a fluid upon agitation, then by using a liquid system the mixer flow can be mapped out. Although the liquid flow will not take into consideration the particulate behaviour and solid mixing behaviour such as segregation[3], it will be representative of any dead spots within the mixer and serve as a precursor to simulations of full multiphase flows.

In order to simulate the mixer flow field, a liquid case was modeled using STAR-CD version 3.22. The model was a laminar flow, this was based on calculation for Reynolds number[3](equation 1) for the original mixer and was scaled using dynamic similarity.

$$Re = \frac{(\rho\, N\, D^2)}{\mu} \tag{1}$$

The flow is then divided into three regimes[3][4](table 1), where;

Region	Regime
Re $\ll$ 100	Laminar
100 $\ll$ *Re* $\ll$ 10000	Transitional
Re $\gg$ 10000	Turbulent

Table 1: Flow regimes

The flow was modeled as a steady state case with a single rotating frame of reference. A single liquid, namely water, was used as the working fluid, rotating at a velocity of 30 rpm. A third of the geometry has been modeled using cyclic boundary conditions, based on the assumption that it is a periodic flow. The initial grid consisted of approximately 500,000 cells. As the flow was incompressible the following equations were solved:

Continuity

$$\frac{\partial u_j}{\partial x_j} = 0 \tag{2}$$

Momentum

$$\frac{\partial u_i}{\partial t} + u_j \frac{\partial u_i}{\partial x_j} + \frac{1}{\rho}\frac{\partial p}{\partial x_j} = \nu \Delta u_i + s_i \tag{3}$$

Where s_i is a user-defined source term. In the case of this model, s_i is the source term due to rotational forces, where;

$$s_i = f\left(u_k, w_k, r_k\right) \tag{4}$$

A SIMPLE upwind scheme was used to solve the conservation equations and the convergence criterion was set at 1×10^{-6}. The data obtained from the single liquid case was validated via a grid independence study with a second grid that consisted of 1.2 million cells. The experimental PIV data was also used to validate the numerical data. Other parameters such as mixer fill and blade location were also investigated.

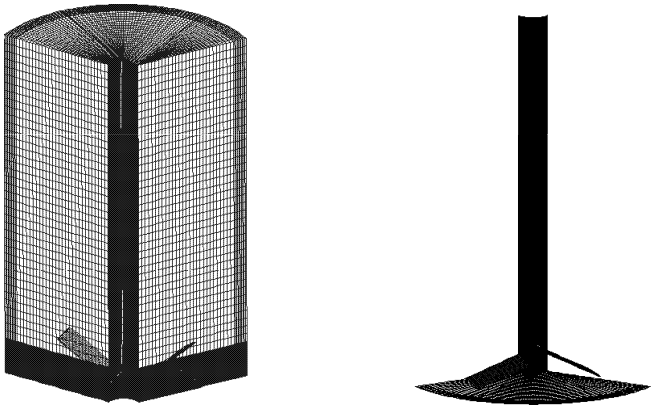

Figure 4: (a)Complex blade mesh (b) Complex mesh internal view

2.2.2 Case B-VOF Case

Once realizable results were obtained from case A, the new blade geometries were simulated with a binary mixture. The single liquid simulations allowed the flow to be mapped within the mixer, identifying any dead spots. The binary mixture will allow us to determine the mixing capabilities of the blade configuration allowing us to see more clearly the true potential of the agitator. For the binary mixture, water and glycerol were used. Although both the liquids have roughly the same density, glycerol is 1000 times more viscous than water. Water and glycerol were used as glycerol is a miscible liquid and would readily mix with water. By keeping viscosity as the only variable, we were able to identify the dead spots and the different modes of rotation.

Having established grid independence, the coarse grid (500,000 cells) was used as it would converge quicker than the finer grid. In order to take account of the interaction between the water and glycerol, a volume of fluid (VOF) model was introduced[6].

Continuity

$$\frac{\partial}{\partial t}\left(\alpha_k \rho_k\right) + \nabla.\left(\alpha_k \rho_k u_k\right) = \sum_{i=1}^{N}\left(\dot{m}_{ki} - \dot{m}_{ki}\right) \qquad (5)$$

Conservation of Momentum

$$\frac{\partial}{\partial t}\left(\alpha_k \rho_k u_k\right) + \nabla.\left(\alpha_k \rho_k u_k u_k\right) - \nabla.\left(\alpha_k \tau_k\right) = -\alpha_k \nabla p + \alpha_k \rho_k g + M \qquad (6)$$

Conservation of Energy

$$\frac{\partial}{\partial t}\left(\alpha_k \rho_k e_k\right) + \nabla.\left(\alpha_k \rho_k u_k e_k\right) - \nabla.\left(\alpha_k \lambda_k \nabla T_k\right) = Q \qquad (7)$$

Where α_k is the volume fraction of phase k, ρ_k is the phase density and u_k is the phase velocity. N is the total number of phases, $\dot{m}_{ki}$ and $\dot{m}_{ki}$ are the mass transfer rates to and from the phase. τ_k is the laminar shear stress, p is the pressure, M is the sum of inter facial forces, e_k is the phase enthalpy, λ_k is the thermal conductivity and Q is the inter facial heat transfer.

Again a SIMPLE upwind scheme. The solutions converged with residuals of approximately 1×10^{-5}. The VOF model solves the conservation equations[6] for each phase.

As both phases are within the same flow domain, they will share a common pressure field. However, other properties such as density, thermal conductivity, velocity and temperature must be defined. The interaction between the phases is taken into account by the additional interphase transfer term M in equation 6.

2.3 Results

2.3.1 Single Liquid Results and Validation

The numerical results from case A showed that most of the mixing occurs in the blade region and that there was very little mixing above and below the blade region. From figure 5 we can see that there are very low velocities above the blade. In the region next to the shaft the flow is moving downwards and in the near wall region on the periphery of the mixing vessel the flow is moving upwards. Indicating some kind of toroidal shape. We can also see the bands of velocity from figure 5, this indicates that there are concentric cylinders of fluid rotating about the shaft where no mixing is taking place between these 'shear'layers.

From figure 6, we can see that there is mixing within the blade region and virtually no mixing above the blade region. This is due to the solid body rotation of the bulk flow above the blade region.

Figure 5 and figure 6 show a good qualitative agreement, as both sets of data indicate the presence of mixing within

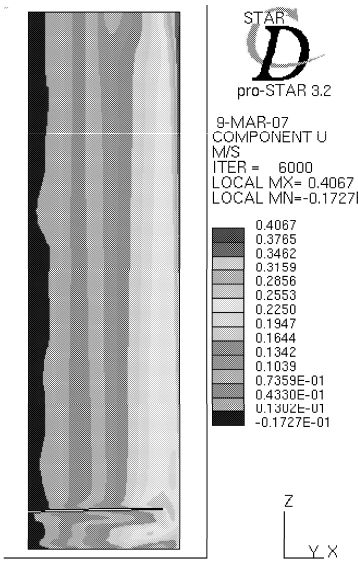

Figure 5: U component plot-numerical data

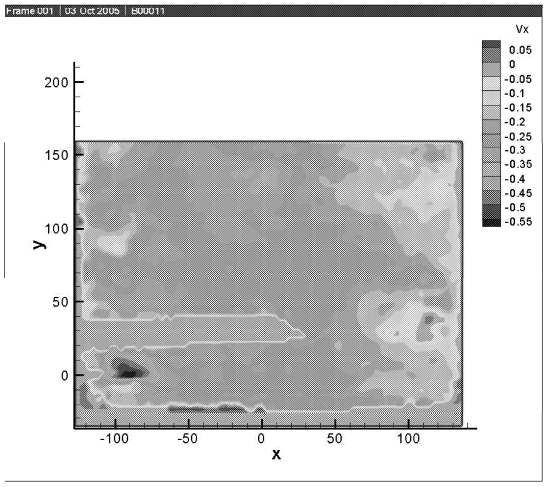

Figure 6: U component plot-experimental data

the blade region and no mixing above the blade region. Both plots also show the velocity present in the near wall region.

2.3.2 VOF Results

As the simulation took a long time to converge, data points were taken at regular intervals to determine the level of mixedness in the flow. Figure 7 shows that the level of mixedness approached zero asymptotically. The simulation was then stopped at 8 seconds simulation time, as the value of mixedness had remained the same for approximately 3 seconds, the VOF case took approximately 4 months to converge. In order to determine the mixture quality from the VOF calculation, we calculated the variance for the cells, defined as;

$$\sigma^2 = \frac{\sum(x - \bar{x})^2}{N} \tag{8}$$

Where x is the sample concentration of the mixture, x is the mean concentration and N is the number of samples. The variance was firstly calculated for the whole mixing vessel. In an ideal binary mixture, the value of the variance should be zero[3][4] and thus for a fully segregated mixture the variance will be 0.25. As the level of mixedness increases the value of the variance decreases.

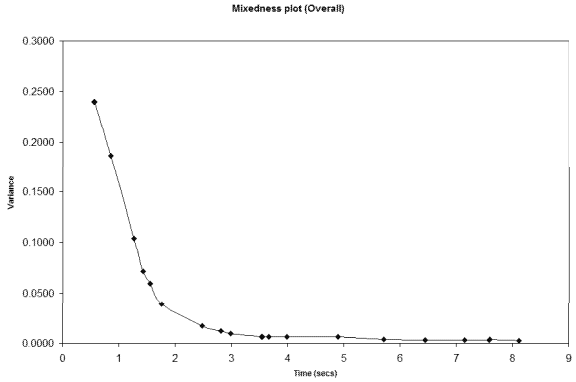

Figure 7: Overall mixedness

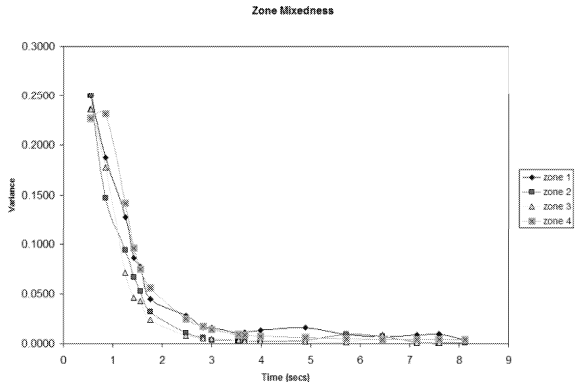

Figure 8: Zone mixedness

In order to determine where this inhomogeneity was located, the mixer was divided into four zones; below the blade (zone 1), the blade section (zone 2), bulk section immediately above the blade (zone 3) and the upper bulk section (zone 4). The variance was calculated for each of the zones (figure 8). Initially, it may seem that all the different zones have the same kind of mixedness, and the inhomogeneity problem may be a global one. However, on close examination, one can see that the highest variance is below the blade (zone 1). This is due to a dead spot under the hub. As the blade is rotating, it will entrain fluid from all directions, except from under the hub as there is no movement of the fluid.

The results from the VOF calculation show that there are two modes of rotation for the fluid; one mode is the

rotation about the x-axis and the second mode is rotating around the periphery, creating a toroidal shape. This can be seen from figures 9(a)-9(d). This toroidal shape corresponds to the flow from the single fluid experiments. From the simulation we can also see an oscillatory motion of the fluid along the shaft. The time of the oscillation is related to the position of the upper blade.

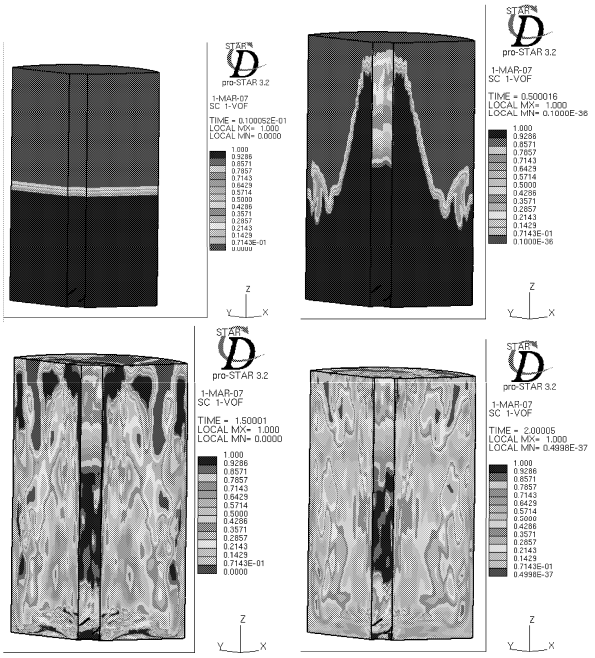

Figure 9: VOF plots at (a)t=0s, (b)t=0.5s, (c)t=1.5s, (d)t=2.0s

3 Conclusions

The numerical and experimental data for the single liquid case are in agreement with each other. Both plots show the presence of mixing in the blade region and the presence of solid body rotation above the blade. The VOF data demonstrated the two modes of mixing are present within the vessel; one about the central axis and one along the periphery. The fluid around the shaft has an oscillatory motion related to the position of the upper blade. The variance of the mixture decreases rapidly within the first two seconds and then asymptotically approaches zero. The variance below the blade (zone 1) is higher than the other zones indicating that there is poor mixing in this region. This is confirmed by the mixer plots (figure 9a- figure 9d), where a region with zero velocity, i.e a dead zone, is present. New agitators have been designed based on theoretical powder mixing. The new blade design has been manufactured and experimental tests will be conducted on the actual mixer. Where solid particles will be mixed and samples will be taken at various positions to determine the level of homogeneity within the mixture. This will be compared with the complex blade, and the efficiencies will be compared.

4 Work in Progress

4.1 Eulerian Two Phase Modeling

The next stage towards understanding solid mixing is to model the solid particles. Initially there are three options, Lagrangian Multiphase modeling (LMM), Eulerian Multiphase modeling (EMM) or Eulerian-Lagrangian Modeling (ELM). Unfortunately, Lagrangian multiphase modeling and Eulerian-Lagrangian modeling would both need significant amounts of computing power and storage, as the constitutive equations would be solved for each particle. This will form the basis of the next stage of computation.

The Eulerian multiphase model[7][6] can be used to model two more phases in a single flow domain, where the phase can be solid, liquid or gas. Examples of multiphase flows are; atomisation, dispersed flows and fluidised beds.

The Eulerian multiphase model treats each phase as individual inter-penetrating continua, unlike the Lagrangian model (where there is one phase is treated as a continua and the dispersed phase is treated as individual particles). Like the free surface flow, conservation equations for mass, energy and momentum are solved for each phase.

4.2 Acknowledgements

The authors would like to Federal Mogul for all their help and advice. We would also like to thank La Vision and TSI for their generosity and help with the PIV experiments. And finally, we would like to thank CD Adapco for all their help and advice.

References

[1] R.L. Stewart, J. Bridgwater, Y.C. Zhou, and A.B. Yu. Simulated and measured flow of granules in a bladed mixer-a detailed comparison. *Chemical Engineering Science*, 56:5457–5471, 2001.

[2] F.J. Muzzio, C.L. Goodridge, A. Alexander, P. Arratia, H. Yang, O. Sudah, and G. Mergen. Sampling and characterisation of pharmaceutical powders and granular blends. *International Journal of Pharmaceutics*, 250:51–64, 2003.

[3] M.E. Edwards, N. Harnby, and A.W. Nienow. *Mixing in the Process Industries*. Butterworth Heinemann, 2001.

[4] E.L. Paul, V.A. Atiemo-Obeng, and S.M. Kresta. *Handbook of Industrial Mixing*. Wiley-Interscience, 2004.

[5] M. Raffel, C. Willert, and J. Kompenhans. *Particle Image Velocimetry, A Practical Guide*. Springer, 1998.

[6] *Star Methodology.* CD-Adapco, Version 3.26.

[7] Simon Lo. Modelling Multiphase flow with an Eulerian Approach. *VKI Lecture Series-Industrial Two-Phase Flow CFD*, 2005.